Ninth Canadian Conference on
Earthquake Engineering
Ottawa, Ontario, Canada
26-29 June 2007

CYCLIC TEST OF CONCRETE BEAMS REINFORCED BY PLAIN BARS

M. S. Marefat[1], R. Rostamshirazi[2], S. M. Hassanzadeh[2], I. Ghorbani[2] and M. Khanmohammadi[3]

ABSTRACT

There are many buildings throughout the world that have been built in the past decades and lacking sufficient seismic details, have been reinforced by plain bars. To predict the response of such buildings under cyclic motion, it is necessary to examine their behavior in the laboratory. In this study, the results of tests of five beams under cyclic and monotonic load are presented. Three beams are reinforced by plain bars and two by deformed bars. The tests show that relatively large slip is a characteristic of cyclic and monotonic responses of beams reinforced by plain bars. The value of slip of smooth bars is almost twice greater than that of deformed bars. Beams reinforced by plain bars suffer about 30% loss of ductility, 10% decline of yield strength, 33% drop of energy absorption capacity relative to those reinforced by deformed bars. But, effective elastic stiffness of two types of beams is the same, with a value of about 25% of the gross concrete stiffness. Crack patterns of specimens reinforced by plain bars is quite different from that of deformed bars. In deformed bar specimens, numerous shear-flexural hair cracks form over the plastic hinge region. In the plain bar specimens, a few relatively wide parallel cracks form, with a relatively regular pattern at a distance of about ¼ to ½ of the depth of section from each other.

Introduction

There are many buildings throughout the world that have been built in the past decades and lacking sufficient seismic details, have been reinforced by plain bars. To predict the response of such buildings under cyclic motion, it is necessary to examine their behavior in the laboratory. There are numerous reports of experimental and theoretical studies that deal with reinforced concrete members with deformed bars (e.g., Jae-Yeol Cho, 2006; Marefat, 2006; Pandey, 2005; Lin, 2005; Patrick, 2004; Nathan, 2002; Eberhard, 2002; and Lehman, 2000), but studies on plain bars are relatively rare. Fabbrocinoa (2004) reported some key aspects of structural models of smooth reinforcement for old-type RC frame. Results of experimental tests on smooth rebars and circular hooks and anchoring devices are also used to discuss some aspects of behavioral models of beam-to-column critical regions. Fabbrocinoa (2007) presented an insight on the assessment of relationships between crack width and reinforcement stress in the critical regions of existing concrete buildings, such as column base or beam–column joints, reinforced with smooth bars. Bond strength results from 252 plain bar pullout specimens have been presented by Feldman (2005). Parameters investigated include: concrete compressive strength, bar size, bar shape, concrete cover, and bar surface roughness. Empirical equations based on test results are presented to predict the maximum and residual average bond stresses for plain bars.

[1] Professor of Civil Eng., School of Civil Eng., University of Tehran, Tehran, Iran, e-mail: mmarefat@ut.ac.ir
[2] MS Graduate of Civil Eng., University of Tehran, Tehran, Iran.
[3] PhD Graduate of Civil Eng., University of Tehran, Tehran, Iran.

In this paper, the results of tests on five concrete beams reinforced by plain bars and deformed bars are presented. The tests show that relatively large slip is a characteristic of cyclic and monotonic responses of beams reinforced by plain bars. The value of slip of smooth bars is almost twice greater than that of deformed bars. The ratio of displacement ductility of deformed bars specimens is about five while this ratio for plain bar specimens is about 3.5. This indicates about 30% loss of ductility for specimen reinforced by plain bars. Initial stiffness of specimens with plain bars does not differ from that of deformed bars.

Test Program

Test Specimens

In total, five beams have been tested, three beams have been reinforced by plain bars (SPC-6, SPC-7 and SPC-8) and two beams have been reinforced by deformed bars (SBC-3, NBC-4). The specimens represent members of five story residential buildings and have been fabricated in half scale. Geometry and member specifications of the reference structure (full scale) and specification of all specimens are presented in Fig.1. Specimen SBC-3 is identical to both SPC-6 and SPC-7, and NBC-4 is similar to SPC-8, except for type of longitudinal bars. All specimens have been tested under cyclic load except for SPC-6 that has been tested under monotonic load. Table 1 shows member specifications of the reference structure; characteristics of materials are given in Table 2.

Table1. Geometry and characteristics of members in the reference building (full scale).

Structural type	Numbers of floors	Average span (m)	Beams dimensions (mm)		f'_c (MPa)	Yield Stress (MPa)
			Floors 1, 2	Floors 3, 4, 5		
residential	5	5 m	400x400	300x400	16	400

Table 2. Properties of material of specimens.

Longitudinal bars				Beam dimensions					f'_c (MPa)	Specimen
Ultimate strain	Ultimate stress (MPa)	Yield strain	Yield stress (MPa)	Area of bars(mm) A's	Area of bars(mm) As	Effective depth (mm)	Length (mm)	Width (mm)		
0.18	510	.0018	370	305	452	175	200	200	23	SBC-3
0.18	510	.0018	370	192	418	125	150	200	14	NBC-4
0.18	490	.0017	356	305	452	175	200	200	29	SPC-6
0.18	490	.0017	356	305	452	175	200	200	25	SPC-7
0.18	490	.0017	356	192	418	125	150	200	25	SPC-8

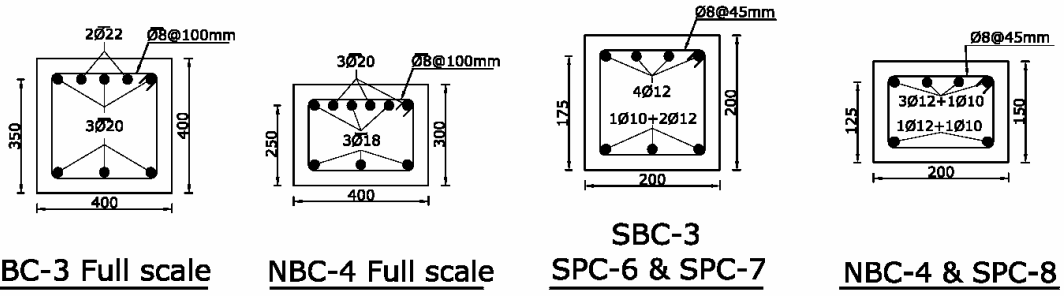

Figure 1. Cross section of beams in the reference building and specimens (dimensions in mm, Φ10 = 78 mm^2 and Φ12 =113 mm^2).

Test Setup and Load Pattern

The test setup is shown in Fig. 2. A horizontal hydraulic actuator, with a capacity of 100 kN, applies load to the free end of the specimen in two opposite directions. Deflection at the top of specimens is measured by the horizontal actuator as well as by an additional horizontal LVDT.

Loads are measured by load cells which are built in the actuators, and several LVDTs record horizontal and vertical displacement at critical sections. Several strain gauges are attached to longitudinal and transverse bars, at different levels, to record the magnitude of strains at different stages. Horizontal loading has been applied in stroke control mode, in a quasi-static manner, and follows a pattern given in Fig. 2.

Behavior of Specimens

In Fig. 3, the force displacement curve of Specimen SPC-8 has been shown. Fig. 4 shows the cyclic response of SPC-6 and the monotonic response of SPC-7. All those specimens have been reinforced by plain bars. The curves demonstrate an initially relatively stiff and linear response before appearance of large displacement stage. At large deformation, the cyclic curves experience relatively sudden drop of both strength and stiffness, but the local drop is followed by a stable resistance and a ductile response. The local decline of strength is not seen in the monotonic behavior but the curve show a relatively good envelop for the cyclic response.

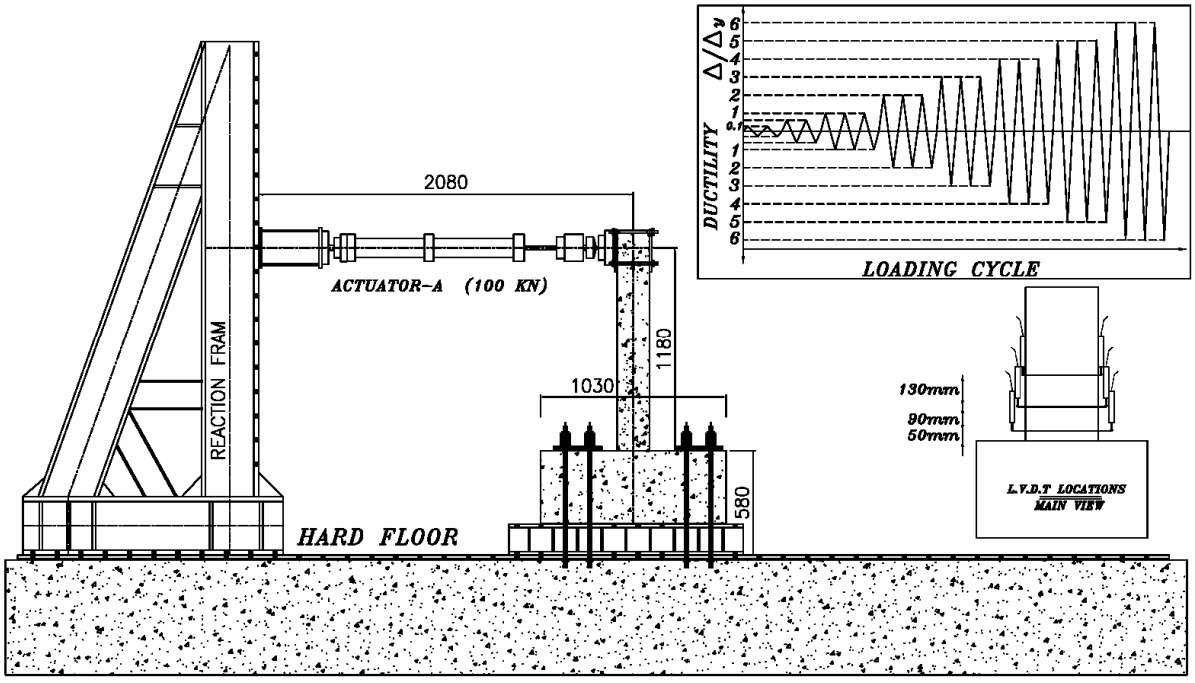

Figure 2. Experimental setup and load pattern.

After yield, the specimens do not show any significant hardening behavior and slope of the curve is less than 2% of initial slope. Relatively considerable slip of longitudinal bars has been a characteristic of specimens reinforced by plain bars as will be discussed. The considerable slip may be the main cause to delay strain hardening of the bars to begin, and hence, any significant increase of strength to appear. In order to idealize the response of specimens, a bilinear curve may be chosen. The idealized curve is shown in Fig. 5.

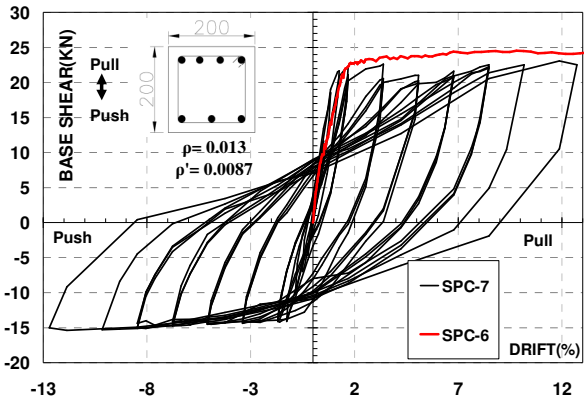

Figure 4. Monotonic curve of SPC-6 and Hystersis curve of SPC-7.

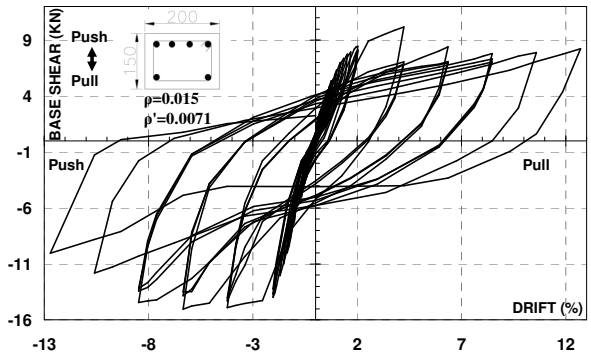

Figure 3. Hystersis curve of SPC-8.

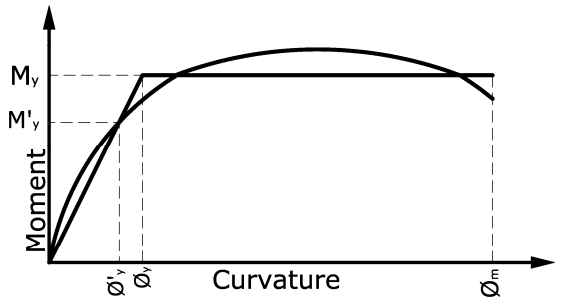

Figure 6. Yield point of member.

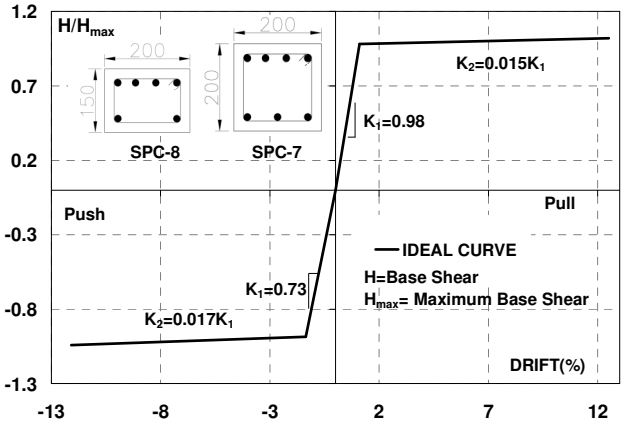

Figure 5. Ideal curve for beams reinforced by plain bars.

Comparison of Specimens with Plain Bars to Specimens with Deformed Bars

Initial Stiffness, Displacement Ductility, and Yield Strength

As mentioned above, two specimens were reinforced by deformed bars to be compared with specimens reinforced by plain bars. The compared specimens were identical in terms of geometric and material characteristics as well as in load pattern. The differences were the type of bar, i.e., plain or deformed bar, yield strength of plain and deformed bar and concrete strength.

In Figs. 7 and 8, the cyclic responses of two types of specimens have been superimposed. In addition, the ratio between effective elastic stiffness, from the test and based on definition of yield point according to Fig. 6, and stiffness of gross concrete section, from calculation, have been shown in Table 3. No visible differences between two types of specimens are observed and all beams show an effective stiffness ratio of about 25% relative to the gross concrete stiffness. It may be said that the initial stiffness of members is mainly a function of geometry of specimen and property of materials rather than the type of bar surface.

To compare with other work, the ratio of effective stiffness that has been recommended for beams by FEMA-356 is equal to 0.5, by ACI-318 is equal to 0.35, and by [Paulay and Priestly 1992] varies between 0.3 to 0.5. The difference between the test result and those recommendations may be related to the difference of behavior of a beam in a frame with that of an individual member (MacGregor, 1993; Timo, 2005; Bardakis, 2007). A number of reports (Elwood, 2006; Telemachos, 2001; Bardakis, 2007) have given almost the same values as those of this test.

Lateral displacement ductility of beams may be expressed by the ductility coefficient according to the following formula: (Clough, 1966; Paulay, 1992)

$$\mu_{\Delta} = \frac{\Delta_u}{\Delta_y} \quad (1)$$

Where Δ_u is lateral displacement at ultimate state and Δ_y is lateral displacement at yield (in accordance with Fig. 6). The ultimate stage has been determined either by 20% drop in strength or buckling of longitudinal bars, whichever takes place first. Other failure modes did not happen in the tests. Table 3 shows that the ratio of displacement ductility of deformed bars specimens is about 5 while this ratio for plain bar specimens is about 3.5. This indicates about 30% loss of ductility if plain bars are used. If monotonic behavior of SPC-6 is compared to cyclic behavior of specimens SPC-7 and SPC-8, much larger ductility ratio, more than two fold, is observed for monotonic response.

Table 3. Ratio of effective stiffness and displacement ductility for different specimens.

Effective stiffness ratio	Ductility ratio		Ultimate drift ratio (%)		Yield drift ratio (%)		Specimens	
$EI_{(test)}/EI_{(gross)}$	μ^{PUSH}	μ^{PULL}	Δ_u^{PUSH}	Δ_u^{PULL}	Δ_y^{PUSH}	Δ_y^{PULL}		
0.26	*5.0*	*4.5*	*12.8*	*11.5*	*2.6*	*2.6*	*SBC-3*	Deformed bar beams
0.27	*5.0*	*5.0*	*14.7*	*9.6*	*2.9*	*1.4*	*NBC-4*	
-	*-*	*7.8*	*-*	*18*	*-*	*1.8*	*SPC-6*	Plain bar beams
0.26	*3.7*	*3.9*	*12.6*	*12.6*	*3.4*	*3.3*	*SPC-7*	
0.25	*3.4*	*2.2*	*7.4*	*4.2*	*2.0*	*2.0*	*SPC-8*	

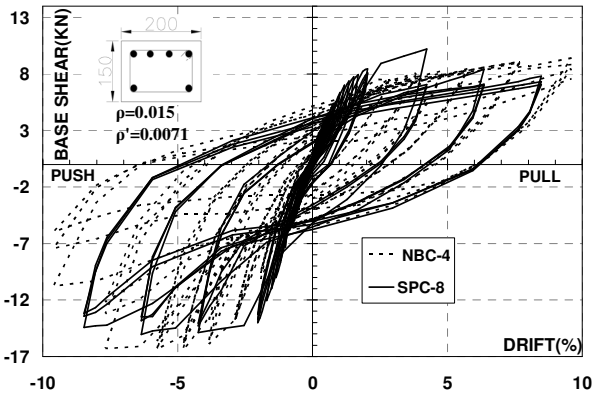

Figure 8. Hystersis curves of NBC-4 (deformed bar) and SPC-8 (plain bar).

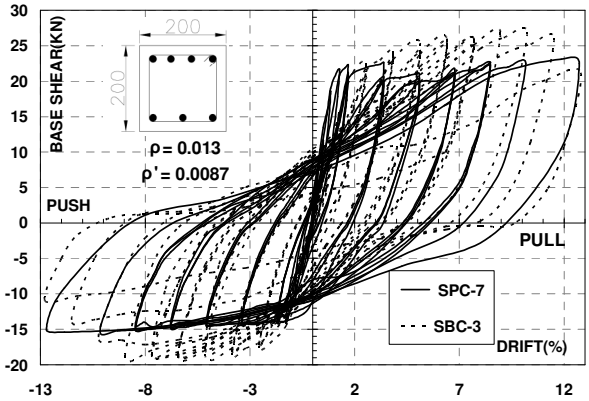

Figure 7. Hystersis curves of SBC-3 (deformed bar) and SPC-7 (plain bar).

Table 4. Yield strength of section and member and energy dissipation capacity for specimens.

Energy dissipation (KN.m)	Yield moment ratio	Yield moment (kN.m)		Specimens	
		Member (test) M_Y	Section (theoretical) M_Y		
25.3	0.92	24.0	25.90	SBC-3	Deformed bar
18.8	0.88	22.5	25.50	SPC-7	Plain bar
8.44	1.10	16.5	15.00	NBC-4	Deformed bar
5.97	0.91	14.8	16.20	SPC-8	Plain bar

Although the initial stiffness of two types of specimens is the same, the yield strengths are different. Figs. 7 and 8 shows that the yield strength of specimens reinforced by plain bars suffers 10% decline relative to the specimens reinforced by deformed bars. Furthermore, if yield of member, from the test, is compared to yield of section, from calculation, the results of Table 4 will be obtained. It is observed that the ratio between the yield moments of member to yield moment of section for specimen reinforced by plain bar varies from 0.88 to 0.91 while this ratio for specimens reinforced by deformed bars is 0.92 to 1.10.

Hysteresis Energy Capacity

Hysteresis curves of Specimen SPC-7, with plain bars, and SBC-3, with deformed bars, are superimposed in Fig. 7. It is seen that the initial response of the specimens is almost similar. But with increase of displacement, Specimen SPC-7 shows considerable pinching, especially, at relatively large deformation. The pinching effect is much less for Specimen SBC-3 with deformed bars. This is anticipated because of slip of smooth bars that cause a decline in the hysteresis loop area. The same comparison is observed for Specimen SPC-8 with plain bar and Specimen NBC-4 with deformed bars, Fig. 8. To quantify energy dissipation capacity, the following formula may be used. The related terms are illustrated in Fig. 9 (Hwang, 2003).

$$E_N = \sum E_i \tag{2}$$

Where E_i is the energy dissipated in each cycle. The calculated values of energy dissipated for different specimens are shown in Table 4. It is seen that specimens reinforced by deformed bars have demonstrated an energy absorption capacity of about 33 % higher than those of plain bars. This is in agreement with other experimental results in terms of slip and crack pattern.

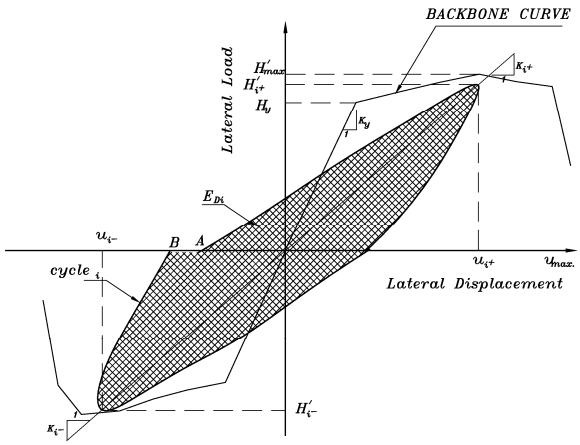

Figure 9. Energy dissipation in each cycle

Slip of Plain Bar

A distinct characteristic of the specimens reinforced by plain bars is the occurrence of a relatively large slip of longitudinal reinforcement (also, see Fabbrocinoa, 2004). According to observation, slip of plain bars has started from the beginning of tests and has increased in an accelerating rate before yielding of specimens. After yield, the magnitude of slip has increased considerably and this has continued to the end of the tests. In order to quantify the magnitude of slip, total deformation of specimens can be divided into three parts, i.e., bending deformation, slip deformation, and shear deformation according to the following formulae (Elwood, 2006).

$$\Delta_{Total} = (\Delta_{Bending} + \Delta_{Slip} + \Delta_{Shear}) \tag{3}$$

$$L = L(M_{Max} - M_y)/M_{Max} \tag{4}$$

$$\Delta_{Bending} = 1/3(\phi_y L^2) + 1/2(\phi_{\max} - \phi_y) L_y (L - L_y/3)$$

$$\Delta_{Slip} = \theta_{Slip} \times L = L(u_t - u_c)/D \quad (5)$$

$$\Delta_{Shear} = VL/(A_{Eff} \times G_{Eff}) \quad (6)$$

Where L denotes the beam length, $\emptyset_y$ and $\emptyset_{max}$ are the yield and maximum curvature, respectively, M_{max} and M_y are the yield and maximum moments, respectively, θ_{slip} is the slip rotation, U_t and U_c are the slip extensions of the two extreme embedded longitudinal bars, D is the distance between the two extreme embedded longitudinal bars, V is the beam shear demand, A_{eff} is the effective shear area, G_{eff} is the effective shear modulus.

The displacement component due to slip can be determined on the basis of deformations recorded by the vertical LVDTs located at the surface of foundation**.** It is assumed that the deformation recorded at this bottom level is primarily the result of strain penetration of the longitudinal steel into the anchor block. Rotation of section can be calculated from dividing the differential displacement of both sides of section by the distance between two LVDTs. Assuming that the beam rotated about its midpoint, the horizontal displacement component due to slip has been obtained by multiplying the calculated rotation by the specimen elevation.

The flexural component has been determined from the displacements measured by four vertical LVDTs at each instrumentation level. First, the measured displacements on both the north side and south side of the specimens were averaged. The difference in the magnitudes of the resulting displacements was divided by the horizontal distance between the north and south LVDTs to obtain the rotation of the specimens at the subject instrumentation level. The flexural displacement component at each instrumentation level was obtained by multiplying one half of the calculated rotation by the vertical distance between instrumentation levels. Cumulative rotations and flexural displacements of lower levels were accounted for in the flexural displacement calculations as the analysis proceeded up the specimen height. Above the uppermost instrumentation level, the flexural displacement component was assumed to vary linearly and was calculated as the sine of the rotation angle measured at the uppermost instrumentation level multiplied by the differential specimen elevation above that level.

Shear displacement can be determined from the deformations measured by the diagonal LVDTs at each instrumentation level. Different studies (Anthony, 2001; Elwood, 2006; Jae-Yeol, 2006) suggest that shear deformation contributes to less than 10% of total displacement. In these tests, diagonal deformation was not measured; therefore, the shear displacement component was not evaluated and unmeasured components plus errors have been labeled as unmeasured.

In Fig. 10, the shares of slip, flexure, and shear in total deformation of Specimen SPC-8, with plain bars, has been illustrated. It is clear that the share of slip is about 60% of total deformation. With increasing drift, the slip portion has increased considerably such that it may account to most of total deformation.

Figs. 11 and 12 show the share of different components in total deformation for two identical specimens SPC-7 and SBC-3 that have been reinforced by plain and deformed bar respectively. According to Fig. 11, the slip of longitudinal bars has started from the beginning of test such that at a drift ratio as small as 0.5%, the portion of slip is three times greater than the portion of flexural deformation. As the drift ratio increases beyond 0.5%, the share of flexural deformation has remained constant but the portion of slip has increased considerably. At a drift ratio of 7%, slip deformation accounts for about 60% of total deformation. The state in Specimen SBC-3 with deformed bars, Fig. 12, is quite different from plain bars. In this specimen, the share of bending deformation is always larger than the share of slip deformation and at relatively large deformation; the two components become almost equal.

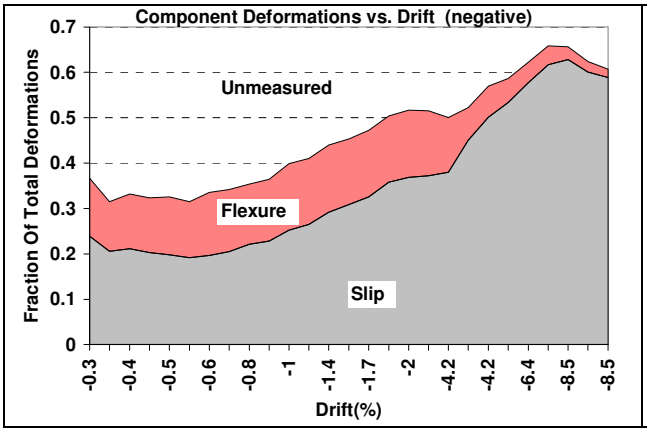

Figure 10. Shares of component deformations, SPC-8.

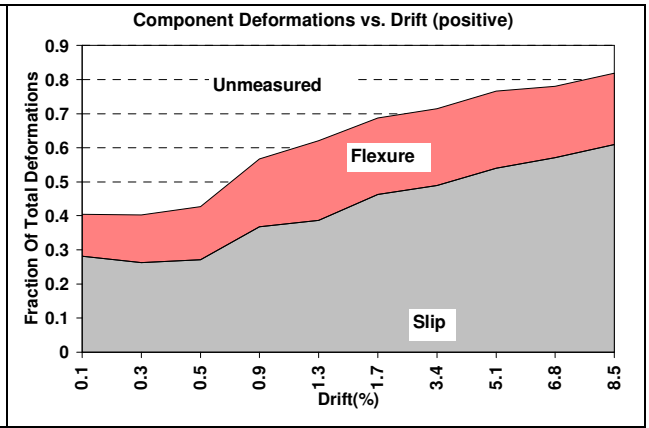

Figure 11. Shares of component deformations, SPC-7.

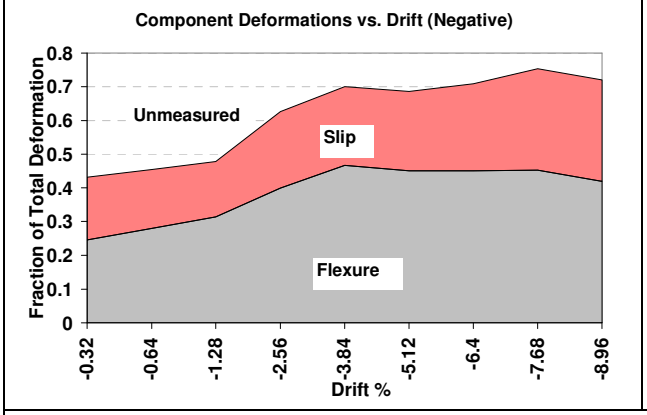

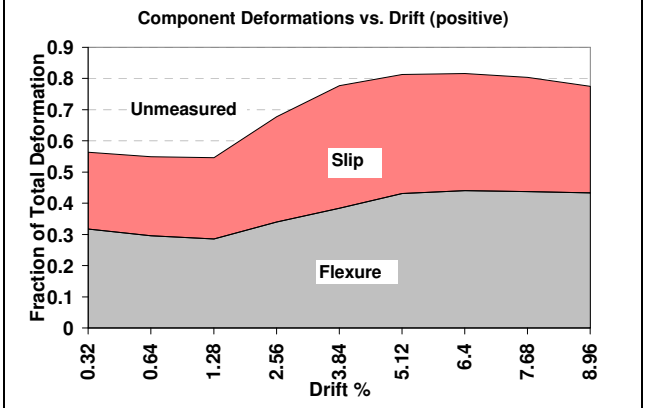

Figure 12. Shares of component deformations, SBC-3.

Crack Pattern

Crack pattern of specimens reinforced by plain bars is quite different from that of deformed bars. Fig. 13 demonstrates the crack pattern of different specimens.

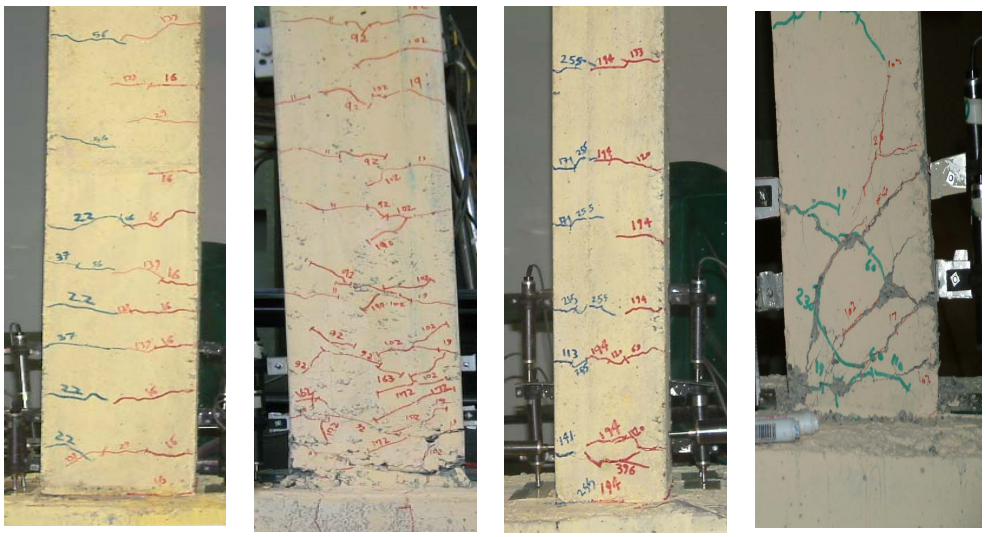

Specimen SPC-7 with plain bar | Specimen SBC-3 with deformed bar | Specimen SPC-8 with plain bar | Specimen NBC-4 with deformed bar

Figure 13. Crack patterns of different specimens.

In deformed bar specimens, numerous hair cracks form over the plastic hinge region, and with increase of lateral displacement, cracks extend to the whole length of specimens. The cracks show a flexural beam type form with straight or inclined orientation relative to the member axis, as is expected for usual reinforced concrete beams [Kemp 1979, Bengtb 1965, Leroy 1967, and Kim 1999].But, in the plain bar specimens, a few relatively wide cracks appear that show a relatively regular pattern.

The cracks extend in parallel at a distance of about ¼ to ½ of depth of section from each other, perpendicular to the beam axis, over a length that does not exceed ¾ lengths of specimens. At final stages of tests, vertical cracks also appear at concrete surface parallel to the longitudinal bars that may be attributed to relatively large slip of longitudinal bars.

Conclusions

In this research the behavior of beams reinforced by plain bars under cyclic and monotonic load has been studied and has been compared to the behavior of beams reinforced by deformed bars. The beams represent members of residential five storey buildings. The tests show that relatively large slip is a characteristic of cyclic and monotonic responses of beams reinforced by plain bars. Slip commences from the very beginning of loading and continues throughout the test and accounts for most of lateral displacement. The value of slip of smooth bars is almost twice greater than that of deformed bars.

The ratio of displacement ductility of deformed bars specimens is about five while this ratio for plain bar specimens is about 3.5. This indicates about 30% loss of ductility for specimen reinforced by plain bars. Initial stiffness of specimens with plain bars does not differ from that of deformed bars. All beams show an effective stiffness ratio of about 25% relative to the gross concrete stiffness. The yield strength of specimens reinforced by plain bars suffer 10% decline relative to the specimens reinforced by deformed bars.

Specimens reinforced by deformed bar has demonstrated an energy absorption capacity of about 33 % higher than those of plain bars. Crack pattern of specimens reinforced by plain bars is quite different from that of deformed bars. In deformed bar specimens, numerous shear-flexural hair cracks form over the plastic hinge region. In the plain bar specimens, a few relatively wide cracks appear that show a relatively regular pattern. The cracks extend parallel to each other, perpendicular to the beam axis, at a distance of about ¼ to ½ of depth of section from each other.

References

Bardakis, V.G. and Dritsos, S.E., 2007. “Evaluation assumption for seismic assessment of existing building,” *Soil Dynamic and Earthquake Engineering* 27, 223-233.

Broms, B. ,1965. “Stress Distribution in Reinforced Concrete Members with Tension Cracks,” *ACI Structural Journal. NO*. 62-65.

Calderone, A. J. , D. E. Lehman and J. P. Moehle, 2001. “Behavior of Reinforced Concrete Bridge Columns Having Varying Aspect Ratios and Varying Lengths of Confinement”. *PEER Report 2000/08*.

Cho, J.-Y. and J. A. Pincheira, 2006. “Inelastic Analysis of Reinforced Concrete Columns with Short Lap Splices Subjected to Reversed Cyclic Loads,” *ACI Structural Journal*. No. 103-S30.

Clough, R. W., 1966. "Effect of stiffness degradation on earthquake ductility requirements." *Rep. No. SEMM 66-16*, Dept. of Civil Engineering, Univ. of California at Berkeley, Berkeley, Calif.

Elwood, K.J. and Eberhard, M.O., 2006. “Effective Stiffness of Reinforced Concrete Columns”. *PEER Research Digest 2006-1*.

Fabbrocinoa, G., Verderameb, G.M. and Manfredib, G., 2004. “Structural models of critical regions in old-type r.c. frames with smooth rebars” *Engineering Structures* 26, 2137–2148.

Fabbrocinoa, G., Verderameb, G.M., Poleseb, M., 2007. “Probabilistic steel stress–crack width relationship in R.C. frames with smooth rebars” *Engineering Structures* 29, 1–10.

Feldman, L. R. and F. M. Bartlett, 2005. “Bond Strength Variability in Pullout Specimens with Plain Reinforcement,” *ACI Structural Journal*. No. 102-S85.

FEMA 356, Federal Emergency Management Agency, Concrete Chapter, California, 1992.

Gould, N. C. and T. G. Harmon, 2002. “Confined Concrete Columns Subjected to Axial Load, Cyclic Shear, and Cyclic Flexure—Part II: Experimental Program,” *ACI Structural Journal*, No. 99-S5.

Heffernan, P. J., M.-A. Erki, and D.L. DuQuesnay, 2004. “Stress Redistribution in Cyclicaly Loaded Reinforced Concrete Beams.” *ACI Structural Journal*, No. 101-S27.

Hwang, S. K. and Yun, H.D., 2003. “Effects of transverse reinforcement on flexural behavior of high strength concrete columns,” Engineering Structures 26 (2004) 1–12.

Kemp, E. L. and Wilhelm, W. J., 1979. “Investigation of the Parameters Influencing Bond Cracking,” *ACI Structural Journal*. NO. 76-3.

Kim, W. and R. N. White, 1999. “Shear-Critical Cracking in Slender Reinforced Concrete Beams,” *ACI Structural Journal*, No. 96-S83.

Lehman, D.E. and Moehle. J.P., 2000. “Seismic Performance of Well Confined Concrete Bridge Columns,” *Pacific Earthquake Engineering Research Center*, University of California, Berkeley,

Lin, C.-H. and S.-P. Lin, 2005. “Flexural Behavior of High-Workability Concrete Columns Under Cyclic Loading,” *ACI Structural Journal*. No. 102-S41.

Lutz, L.A., N. K. Sharma and P. Gergly, 1967. “Increase in Crack Width in Reinforced Concrete Beams under Sustained Loading,” *ACI Structural Journal*. NO. 64-45.

MacGregor, G. J., 1993. “Design of Slender Concrete Columns-Revisited.” *ACI Structural Journals*, No.90-S32.

Marefat, M.S., Khanmohammadi, M., Bahrani, M.K, Goli, A., 2006. “Experimental Assessment of Reinforced Concrete Columns with Deficient Seismic Details under Cyclic Load,” *Advances in Structural Engineering*, V. 9, No. 3.

Marefat, M.S., Khanmohammadi, M., Bahrani, M.K, Goli, A., 2006. “Cyclic load testing and numerical modeling of concrete columns with substandard seismic details,” *Computers and Concrete*,” V. 2, No. 5 (2005) 367-380.

Panagiotakos, T. B. and M. N. Fardis, 2001. “Deformations of Reinforced Concrete Members at yielding and Ultimate,”. *ACI Structural Journal*, No. 98-S13.

Pandey, G. R. and H. Mutsuyoshi, 2005. “Seismic Performance of Reinforced Concrete Piers with Bond-Controlled Reinforcements,” *ACI Structural Journal*. No. 102-S30.

Paulay, T. and Priestly, M.J.N., 1992. “*Seismic Design of Reinforced Concrete and Masonry Buildings*“, John Wiley and Sons, New York.

Tikka, T. K. and S. Ali Mirza, 2005. “Nonlinear EI Equation for Slender Reinforced Concrete Columns,” *ACI Structural Journal*. No. 102-S85.